Naval Research Laboratory
Washington, DC 20375-5320

NRL/MR/6720--96-7868

Lithium Hydride Debris Shields for Plasma Radiation Sources

R.E. TERRY

Radiation Hydrodynamics Branch
Plasma Physics Division

September 4, 1996

DISCLAIMER NOTICE

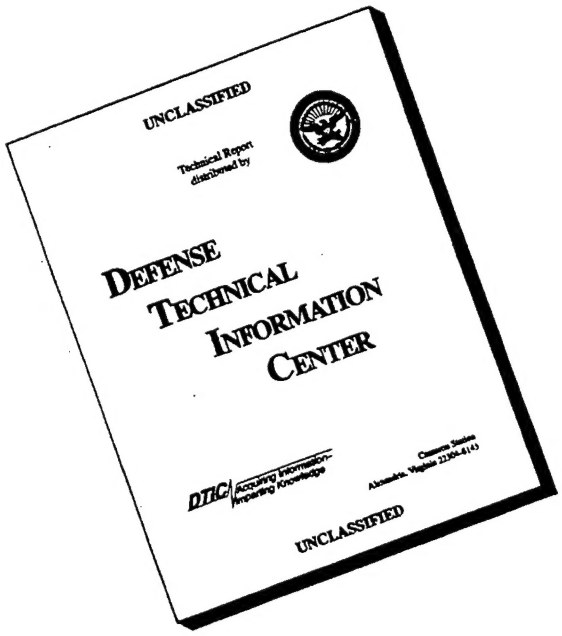

THIS DOCUMENT IS BEST QUALITY AVAILABLE. THE COPY FURNISHED TO DTIC CONTAINED A SIGNIFICANT NUMBER OF PAGES WHICH DO NOT REPRODUCE LEGIBLY.

REPORT DOCUMENTATION PAGE

Form Approved
OMB No. 0704-0188

1. AGENCY USE ONLY (*Leave Blank*)	2. REPORT DATE	3. REPORT TYPE AND DATES COVERED
	September 4, 1996	

4. TITLE AND SUBTITLE

Lithium Hydride Debris Shields for Plasma Radiation Sources

5. FUNDING NUMBERS

6. AUTHOR(S)

R.E. Terry
Radiation Hydrodynamics Branch

7. PERFORMING ORGANIZATION NAME(S) AND ADDRESS(ES)

Naval Research Laboratory
Washington, DC 20375-5320

8. PERFORMING ORGANIZATION REPORT NUMBER

NRL/MR/6720--96-7868

9. SPONSORING/MONITORING AGENCY NAME(S) AND ADDRESS(ES)

Defense Special
Weapons Agency
EST
Alexandria, VA 22310

10. SPONSORING/MONITORING AGENCY REPORT NUMBER

11. SUPPLEMENTARY NOTES

This research was sponsored by the Defense Special Weapons agency under Job Order Title, "NRL Advanced Radiation Theory Support," MIPR No. 95-2062.

12a. DISTRIBUTION/AVAILABILITY STATEMENT

Approved for public release; distribution unlimited.

12b. DISTRIBUTION CODE

13. ABSTRACT (*Maximum 200 words*)

The use of lithium hydride (LiH) for both return current structures and initial debris shielding is explored and a general set of design criteria is derived. It is found that, particularly when the testing requirement is for argon K shell radiation, LiH shields can improve the expected fluence on a test object over present or recently proposed technologies. The concept rests upon a tradeoff between the proximity of a test object to the plasma radiation source (PRS) and the opacity of any shielding that is interposed. Because a larger mass of intervening shield material is possible with LiH, the expected debris velocities are 100 times or more slower than current measurements. A cold press technique for the fabrication of the shield and its electrical connection to a pulser is specified.

14. SUBJECT TERMS

Lithium hydride
Debris mitigation
PRS return current geometry

15. NUMBER OF PAGES

25

16. PRICE CODE

17. SECURITY CLASSIFICATION OF REPORT	18. SECURITY CLASSIFICATION OF THIS PAGE	19. SECURITY CLASSIFICATION OF ABSTRACT	20. LIMITATION OF ABSTRACT
UNCLASSIFIED	UNCLASSIFIED	UNCLASSIFIED	UL

Table of Contents

Lithium Hydride Debris Shields for Plasma Radiation Sources

EXECUTIVE SUMMARY

The use of lithium hydride (LiH) for both return current structures and initial debris shielding is explored and a general set of design criteria is derived. It is found that, particularly when the testing requirement is for argon K shell radiation, LiH shields can improve the expected fluence on a test object over present or recently proposed technologies. The concept rests upon a tradeoff between the proximity of a test object to the plasma radiation source (PRS) and the opacity of any shielding that is interposed. Because a larger mass of intervening shield material is possible with LiH, the expected debris velocities are 100 times or more slower than current measurements. A cold press technique for the fabrication of the shield and its electrical connection to a pulser is specified.

I. MOTIVATION

In any cold x-ray simulator geometry fielded to date, the pinch debris has always played a major role in fixing the proximity of test objects[1,2]. The use of open return current structures formed by metal rods and wire anode meshes allows a very strong plasma wind to emerge from the implosion region and, if uncontained, to damage test objects through unintended processes. Moreover the azimuthal modulation of the pinch forces set up by discrete return current rods can be detrimental to the stability of the PRS implosion. Extensive research efforts[3,4,5,6,7,8] have been expended to stop the debris once it is launched, but all of these schemes involve relatively complex external systems and none offer the possibility of azimuthal smoothing of the pinch forces. By placing a sufficient thickness of conducting, low atomic number material as a window between the plasma radiator and the test object, the task of debris mitigation can be helped in two ways. First, a conducting window will allow an azimuthal smoothing of the implosion forces to minimize the accumlated distortions of the pinch as assembly progresses. Secondly, the window can stop the debris before it is launched, or (more likely) delay the launch of debris sufficiently to have a useful impact on the timing of exterior, mechanical debris mitigation systems.

Low atomic number forces the consideration of rather unconventional substances as debris

shields. The use of such materials is normally avoided in simulator technology. It is considered here because the benefits can clearly be seen to outweigh the (very minor) challenges, provided that some reasonable materials protocols are developed and implemented. In the present work the unconventional material of interest is lithium hydride (LiH) and the basic shape is a cylindrical array (either of solid material or of windows held by metal frames) that replaces the usual return current rods.

A. Stress Demodulation

Current research[9,10,11] has indicated that azimuthal asymmetries play a noticeable role in the dynamics of wire array implosions, perhaps in part because of the regular spacing of return current posts in the PRS diodes. Some experience with more complex systems like the tandem puff at Maxwell Laboratories indicates that strong azimuthal perturbations in the radial progression of the implosion can also occur and are usually disasterous with respect to radiation production.

It is easy to see that azimuthal modulation of the stress on a current element from a regular set of return current paths can produce a perturbation similar to the classic flute mode in theta pinches. The pairwise stress on a single wire from each of $\mathcal{M}$ return paths can be written

$$\mu\ddot{\mathbf{r}} = \Sigma_{m=1}^{\mathcal{M}} \frac{2I_{wire}I_m\hat{\mathbf{r}}_{wm}}{c^2|\mathbf{r}_{wire} - \mathbf{r}_m|} ,$$

with the unit vector in the direction of the wire location. Expanding the force into explicit rectangular components, and specializing to the case of $\mathcal{M}$ return current rods at equally spaced locations and a constant radius, viz $\theta_m = \frac{2\pi}{\mathcal{M}}m$ and $\mathbf{r}_m = R$, the force components can be written

$$\mu\ddot{\mathbf{r}} = \Sigma_{m=1}^{\mathcal{M}} \frac{2I_{wire}I_{out}}{\mathcal{M}c^2|\mathbf{r}_{wm}|}(\mathcal{P}_x\hat{\mathbf{x}} + \mathcal{P}_y\hat{\mathbf{y}}) ;$$

here the projectors are given by

$$\mathcal{P}_x \equiv \cos A\cos\theta_m - \sin A\sin\theta_m ,$$

$$\mathcal{P}_y \equiv \cos A\sin\theta_m + \sin A\cos\theta_m .$$

If the radial or azimuthal component of the cage to wire force is desired, then the equivalent expression becomes

$$\mu\ddot{\mathbf{r}} = \Sigma_{m=1}^{\mathcal{M}} \frac{2I_{wire}I_{out}}{\mathcal{M}c^2|\mathbf{r}_{wm}|}(\cos A\hat{\mathbf{r}} + \sin A\hat{\theta}) ,$$

with the common subexpressions $\cos A$, $\sin A$, and r_{wm} given by

$$\sin A = \sin(\theta_w - \theta_m)\frac{r_m}{r_{wm}} ,$$

$$\cos A = \frac{r_{wm}^2 + r_w^2 - r_m^2}{2r_w r_{wm}} ,$$

$$r_{wm} = \sqrt{r_w^2 + r_m^2 - 2r_w r_m \cos(\theta_w - \theta_m)} .$$

When the radial force is examined as a function of the number of posts involved, the cage array exerts a rapidly diminishing influence on the test wire for a progressively smoother current return structure. The effect is illustrated in Fig. I.1, showing a larger area of essentially zero "cage to wire" force as the number increases. In the limit of a continuous return current structure, the cage exerts no explicit stress on the wire array — its proximity influences only the magnitude of the current by determining the inductance.

B. Debris Mitigation

Recent measurements[12] have established a generic range of PRS debris speeds on the order of 1 to 10 cm/μs, and a typical outward pressure value on a return current element would be about 0.5 kbar at a few ($\approx$6cm) and 3.5 MA of current. Of course the pressure inference assumes that the exterior element can indeed carry circuit current and scales as B^2, viz. $p = p_{sc} \cdot (\frac{Ir_{sc}}{rI_{sc}})^2$.

A general tradeoff between debris shield thickness, valve closure time, and the placement radius for a test object can be easily derived when it is assumed that the full mass of a debris shield is to be accelerated outward. As a debris shield thins, the energy in the pinch cavity would tend to leak through, whether by conduction or shock followed by spalation, and debris matter would thus achieve the high speeds discussed above. The resulting fast component may represent only a few

percent of the shield mass, but it will determine the space and time scale for any mechanical closure devices.

Fixing the closure time for any fast valve technology of interest at τ_c, and assuming that the PRS generates a current pulse only over a characteristic time τ_p, the minimum radial separation between the (inner) debris shield radius and the (outer) test radius where a final closing valve is located is just given by the flight time, viz. $r_{test} - r_0 = \tau_c v_{debris}$. But v_{debris} is set by the outward magnetic pressure and the pulse time, viz. $v_{debris} \geq \frac{p_{sc}\tau_p}{\rho\mathcal{T}} \cdot (\frac{Ir_{sc}}{rI_{sc}})^2$, $\mathcal{T}$ is the shield thickness and ρ is the shield mass density.

Of course that minimum radial separation costs radiative fluence, by a factor $(r_0/r_{test})^2$, while a thicker shield diminishes the fluence exponentially, $\exp -[\mu\mathcal{T}]$. As an estimate of the available radiative intensity at the test radius compared with that at the shield radius, one may write

$$\mathcal{I}_{test}(\nu) \approx \mathcal{I}_0(\nu) \cdot \frac{\exp -[\mu(\nu)\mathcal{T}]}{\left(1 + \frac{\tau_c p_{sc}\tau_p}{\rho\mathcal{T}r_0} \cdot (\frac{Ir_{sc}}{rI_{sc}})^2\right)^2} ,$$

and the two limiting cases are obvious. Conventional technology accepts the fast speeds from thin shields and pays with the radial factor. The shield proposed here selects an attenuating material that is sufficiently translucent at the frequencies of interest for the Ar K shell and optimizes the useable fluence with *both* factors.

To be a clear improvement over existing debris shield materials any LiH return current assembly must be massive enough to withstand such a pressure and still offer a slower rate of expansion, yet translucent enough to minimize its absorption of the incident radiation. The following discussion treats the pros and cons of the LiH return current cage on a topical basis and then suggests a design option.

II. USEFUL LiH PROPERTIES

In other technologies[13,14,15] lithium hydride has been found to be most attractive as a thermal storage medium, a thermal working fluid, and a fuel cell component. A rather extensive industrial and technological experience base exists in aeronautical and astronautical applications, to include

for example the use of *molten* LiH as a heat transfer agent in spacecraft cooling systems. In the present context four properties — heat capacity, thermal conductivity, electrical conductivity, and x-ray opacity — offer the primary basis for a useful addition to PRS simulators.

A. Heat Capacity

Lithium hydride has no competition with respect to heat absorption capacity in the temperature range from 25 to 800 °C. Over this temperature range the substance can absorb 60.235 kJ/mole, including the heat of fusion (21.938±0.942 kJ/mole); and further heating up to the dissociation point will absorb an additional 83.204 kJ/mole. This overall heat absorption capacity is about 35 % greater than that of pressurized water.

Calculation of the heat capacity $c_V(T)$ of crystalline LiH on the basis of a superposition of the acoustic and optical lattice vibrations makes it possible to determine the heat capacity even in the temperature region between 0 and 100 °K where the characteristic acoustic temperature changes considerably (880 °K at T=0 °K → 600 °K at T=100 °K). The only region where this method fails is in a narrow band from 5→15 °K where the heat capacity shows an experimentally measured peak at ≈11 °K.

Above 100 °K the observed behavior is quite successfully calculated by a mixture of heat capacities from acoustic and optical crystal excitation modes, viz.

$$c_V(T) = 3\mathcal{D}(\frac{\Theta_{ac}}{T}) + \mathcal{E}(\frac{\Theta_{LO}}{T}) + 2\mathcal{E}(\frac{\Theta_{TO}}{T})$$

with the longitudinal optical ("LO") and tranverse optical ("TO") branches showing distinct characteristic temperatures. The special functions are the usual Debye and Einstein functions.

Table I. Coefficients for LiH Heat Capacity

m	b_m
0	27.08
1	$1.09078\ 10^{-1}$
2	$-2.79615\ 10^{-4}$
3	$4.74755\ 10^{-7}$
4	$-2.93547\ 10^{-10}$
5	$5.59545\ 10^{-14}$

Above 298.15 °K, the heat capacity is well represented for numerical work by the expression[16]

$$c_p(T) = b_0 + \Sigma_{m=1}^{5} b_m (T - 280\ ^oK)^m\ [J/mole\ ^oK]$$

with the coefficients as shown in Table I. The experimental values for the quantity C_p are shown in Fig. II.1, which also shows the density of the material over the same temperature range.

If one constructs a right circular cylinder of LiH, with a mean thickness δr of a few milimeters, then the energy required to vaporize the structure fully can be written as

$$\mathcal{Q}_{vap} = 175.74(\frac{\delta r}{0.1}\frac{d}{10}\frac{\mathcal{L}}{4})[1 + \frac{\delta r}{d}]kJ$$

and thus a 1mm shell 4 cm long at a 10 cm diameter would require 177.49 kJ of energy to dissociate into vapor. As will become apparent, the expected energy deposition into such a structure during a PRS shot would be orders of magnitude smaller than this *minimum*, implying that the debris from the structure will be created by *mechanical disruption alone*! Since the resulting powder can be accelerated only over a timescale characteristic of the magnetic pressure pulse, the expected debris velocity will be much slower than the sonic speeds characteristic of ejected load gas or partially vaporized material from return current rods. The very favorable combination of high heat capacity and low x-ray opacity puts LiH in a strong position to exploit the debris mitigation tradeoff discussed in Section IB.

B. Thermal Conductivity

As a complement to the hydride's ability to absorb heat, one finds a very poor thermal conductivity, so that heated regions tend to persist, and very thin hot layers can be sustained — particularly over the timescales associated with a PRS implosion. The conductivity also drops with increased temperature, at least for the crystalline material, also acting to keep heated regions localized. The thermal conductivity in crystalline or pressed LiH, $\lambda(T)$ [J/s m °K], is shown in Fig. II.2, and can be represented reasonably well below the melt point with a simple inverse temperature dependence[17] $\lambda_{cr}(T) = 1.51 + 6.4062\ (298.15/T)$.

Using a reference temperature T_0 at about room temperature and the well verified inverse temperature dependence for the thermal conductivity, but neglecting the weak density dependence on

temperature, the equation of thermal transfer in crystalline LiH can be cast in the following form:

$$\partial_t \frac{T}{T_0} = \frac{3.36210^{-5}}{r[1+0.586\frac{T}{T_0}]}\partial_r \left(r[1.51+6.4062\frac{T_0}{T}]\partial_r \frac{T}{T_0} \right) ,$$

and this implies a very inefficient thermal transfer. Consider, for example, an exponential temperature profile, falling with radius at 5.0 cm. If the radial scale height is on the order of 0.1mm, then the fractional change in local temperature over a pinch time of 200ns is only 6.8 10^{-10}!

The only way such an LiH layer can be heated effectively is through direct radiative transfer, not thermal conduction through the solid. Low energy VUV and X-ray spectral components will be absorbed in the material closest to the source, but even if blocked completely, these spectral components would not contain enough energy to vaporize the LiH, except perhaps on the very largest machines.

C. Electrical Conductivity

With an exponentially decaying current layer of skin depth δ, the effective current carrying area in a right circular cylinder can be approximated by the factor

$$\mathcal{A} = \int_{r_i}^{r_i+d} dr 2\pi r \exp -(\frac{r-r_i}{\delta}) = 2\pi[(1-\exp -(\frac{d}{\delta}))](r_i\delta+\delta^2) - d\delta \exp -(\frac{d}{\delta})]$$

with an implied resistance for such a shell given by

$$R_{cyl} = \eta_0 \frac{10 l_p}{\mathcal{A}} \Omega ,$$

with η_0 representing the resistivity of the body.

The electrical conductivity[18] of LiH at a few hundred degrees Celsius is moderate ($2.65 \cdot 10^{-4}$ $[\Omega \text{ cm}]^{-1}$), while that of a layer of metallic Li is quite high ($1.1701 \cdot 10^5$ $[\Omega \text{ cm}]^{-1}$). A simple estimate reveals that, over the course of a typical implosion, the resistor formed by a two skin depth metallic Li layer would receive almost no Ohmic heating ($2.65 \cdot 10^{-8}$[J]). The comparable resistor formed of LiH would receive perhaps, a few millijoules of energy. Clearly, given the large energy

requirements to vaporize or even to melt the LiH crystal phase, such heating will be completely insignificant. If confined to a very thin layer one would expect a largely hydrogen plasma to be formed on any interior, current carrying surface but, apart from helping to symmetrize the return current path even more, this too will have no significant impact on the energy delivered to the LiH debris shield.

D. X-ray Opacity

It is here that LiH really shines as a useful material. Compared to pure Li metal, the hydride actually adds scattering centers per unit volume because of its higher density. On the other hand, the density increase in the hydride occurs because of the very tight chemical bonding that produces, as compared with the pure metal, a roughly two fold increase in the hydride's melting point and a seven fold increase in the heat of fusion. The slightly greater opacity is therefore more than offset by the useful caloric properties which allow milimeter thicknesses to achieve the required energy buffering and still retain substantial translucency to Ar K shell. The opacity has two components[19] — photoelectric and Klein-Nishina, subscripted "ph" and "kn" respectively. A composite material is always blended using the mass fractions, e.g. $\mathcal{A}_{lk} = f_{Li}A_{lk}^{Li} + f_H A_{lk}^{H}$, and then the attenuation is represented by a power law

$$\mu_{ph} = \rho_{LiH} \cdot [\Sigma_{k=1}^{4} \mathcal{A}_{lk} \mathcal{E}_l^{-k}] \,,$$

or a rational function

$$\mu_{kn} = 0.4006 \rho_{LiH} (\frac{\bar{Z}}{A}) \cdot [\frac{1 + A_1 x + A_2 x^2}{1 + A_3 x + A_4 x^2 + A_5 x^3}] \,.$$

The blended coefficients for LiH are shown in the two tables; $\mathcal{E}$ is the photon energy in keV, while $x = \mathcal{E}/511.006$ keV, the photon energy relative to the electron rest mass energy.

Table IVa. Coefficients for LiH Photoelectric Opacity μ_{ph}

$\mathcal{A}_{lk}$	l=1	l=2	l=3
k=1	16.138625	3.83767	0.0354975
k=2	15.63025	44.690075	2.574045
k=3	209.7675	267.9055	113.49825
k=4	8.47617625	26.631875	160.64175

Table IVb. Coefficients for LiH Incoherent Scattering Opacity μ_{kn}

term	value
A_1	1.148
A_2	$6.141\ 10^{-2}$
A_3	3.171
A_4	$9.328\ 10^{-1}$
A_5	$2.572\ 10^{-2}$

The resulting transmission coefficient $T(\mathcal{T},\nu_k) = \exp -\mu(\nu) \cdot \mathcal{T}$ is shown in the table below for seven energies spanning the Ar K shell. Thicknesses up to 3 mm of LiH are considered because the slow debris speeds anticipated should allow one to place the test object half (perhaps even a quarter) as close as is presently done, enhancing the unattenuated fluence by a factor of four or even sixteen.

Table IVc. LiH Transmission of the Ar K shell Radiation

$T(\mathcal{T},\nu_k)$	[kev]	$\rightarrow$					
$\downarrow$ [cm]	3000	3250	3500	3750	4000	4250	4500
.100	.62290	.69389	.74960	.79315	.82721	.85408	.87546
.125	.55338	.63330	.69749	.74851	.78889	.82106	.84682
.150	.49162	.57801	.64900	.70638	.75236	.78931	.81913
.175	.43675	.52754	.60388	.66661	.71751	.75879	.79234
.200	.38801	.48148	.56190	.62909	.68427	.72945	.76642
.225	.34470	.43944	.52284	.59368	.65258	.70125	.74136
.250	.30623	.40107	.48649	.56026	.62235	.67414	.71711
.275	.27205	.36606	.45267	.52873	.59353	.64807	.69366
.300	.24169	.33410	.42120	.49897	.56604	.62301	.67097

The net result is that one could do about as well as present systems, for thick debris shields at the lowest K shell energies, and do substantially better elsewhere!

III. LiH PROPERTIES REQUIRING SPECIAL ATTENTION

A. Reactivity

Lithium hydride dust is extremely irritating to the mucous membranes and skin, causing allergic skin reactions in some individuals. All effects associated with the inhalation toxicity appear to be those due to alkilinity[20]. Finely powdered LiH reacts rapidly with air of low humidity, forming

Li_2O, LiOH, and Li_2CO_3. In moist air the powder may ignite spontaneously and burn fiercely, forming a mixture of products including some nitrogenous compounds. Consequently, LiH dust is apt to explode in humid or even relatively dry air, and transfers of the powdered material should be carried out in an inert atmosphere.

The lump material reacts with humid air to form a superficial coating which inhibits further reaction — several hours exposure of a small cube does not cause appreciable loss of hydrogen , although the "tarnish" is quite evident. Still, lump hydride must not be moistened or exposed to flame. Burning LiH is best extinguished by covering with an inverted can or pail, smothering with *bone dry* graphite powder, or smothering with dolomite. Smothering with sand, especially if moist, can cause explosion. The use of carbon dioxide, carbon tetrachloride, or aqueous fire extinguishers may also lead to explosion.

Containers for the hydride[21] should be fabricated from 347 stainless steel because this material offers the options of storage and heating in the same vessel, due to a low diffusion loss for hydrogen and a very good corrosion resistance to the molten hydride at temperatures below 1050 °C. Corrosion from molten LiH may be significantly enhanced by the presence of oxygen or chlorine impurities — lithium oxide and lithium chloride are extremely corrosive to most metals and ceramics. If a container is to be welded, then atomic hydrogen welds are recommended. Careful attention should be given to the removal of any pockets of flux should any other techniques be used.

B. Adhesion

The solidification of molten LiH is accompanied by significant shrinkage (16 %) , the primary reason being a rather large thermal expansion coefficient[22] for LiH. Combined with a tenacious adherence to the container, this effect can cause castings to crack as they cool. Various materials have been explored which act as lubricants to the die or mold body, and electroplated iron on graphite[23] has been found to be effective.

IV. DESIGN AND FABRICATION

When compared to conventional debris mitigation technology a lithium hydride enclosure is quite competitive. Using fast valve, or shutter techniques, one concedes the fast debris speeds from

thin UV shields and pays the price of containment with a strong radial scaling factor — adding perhaps 10 to 20 cm of excess path length to the interior radius of the return current posts. The shield proposed here selects LiH as an attenuating material that is sufficiently translucent at the frequencies of interest for the K shell of Ar and optimizes the useable fluence with both attenuation and proximity — the final distance added, from return current radius to test object radius, can probably be made 5 cm or less. Unlike any other debris systems yet fielded, the continuous return current surface offers at least the possibility of enhanced yield and reliability because the load stresses are symmetrized. As simulators are scaled to larger initial PRS radii for better electrical coupling, load implosion speed, and the better x-ray yield that is implied, the early symmetry of implosion forces will play a progressively more important role.

A. A Configuration for Ar K shell

A detailed drawing of such a structure is shown in Fig. IV.1a, the general dimensions are appropriate to the lower range of initial radii for either the ACE4 or Decade PRS configurations. In this realization of the scheme, copper rings on either ends of the hydride cylinder provide electrical contact with the MITL electrode (usually the anode) and with the terminating screen anode. To further ensure good electrical contact, the interior of the hydride cylinder is shown coated with a thin (0.1 mm) layer of metallic lithium, providing an initial resistance of $\approx$2.7 mΩ at the 10MHz frequency characteristic of typical pulse power drivers. Since the gas delivery time greatly exceeds both the pulse time and the implosion time, a screen anode that allows the gas load to be vented as the firing pulse erects is always used.

The thickness of hydride shown in this design is well suited to test operations concentrating on irradiation with x-rays at 3 keV and above. Depending on energy only $24 \rightarrow 67$ % of the radiation incident on the shield from the PRS will be transmitted, but the mass of the shield allows debris velocities only on the order of $1 \rightarrow 10 \cdot 10^3$cm/s. A test object can therefore be placed as close as $0.5 \rightarrow 5$ cm away, assuming a closure time in the $\approx$0.5 ms domain for a thin, fast shutter.

Compared to the 10 to 20 cm pathlength required in present technology, this represents an $\approx$ 16-fold increase in the available fluence and therefore yields a net improvement at the test ob-

ject. Clearly, thinner LiH cylinders can do even better, limited by the practical constraints on their strength. For very thin cylinders axial buttresses, mounted outside the anode and MITL rings and equally spaced azimuthally, could be used to relieve the stress on the hydride cylinder arising from support of the end rings.

Another useful alternative is the use of a helical winding of lithium strips on the interior surface of the structure to produce axial fields in the PRS cavity during the early phases of the implosion. As shown in Fig. IV.1b, the number of such strips should be about 20 or more to minimize the azimuthal modulation of the stress pattern on the load, c.f. Fig. I.1, and the axial fields produced can be adjusted in strength with the helical pitch angle. The lifetime of such fields will then depend on how fast the underlying hydride fills in the gaps with hydrogen plasma during the power pulse, but the axial field strategy is primarily useful only early in the implosion because it helps the load build motional impedance sooner than a pure z-pinch. A quicker increase in load impedance allows the load to extract more energy from the pulser at an earlier time.

B. Cold Press Fabrication

Early work[23] in pressed LiH seems to have concentrated on hot pressing at about 600 °C and 1500 psi. Under these conditions there is some opportunity for optimization in the final density obtained by changing the mixture of particle sizes used in the die. Graphite dies are usually effective, particularly when electroplated with iron to minimize the adhesion of the compact to the die material. It is, in fact, the pressure limitations on the graphite which determine the operating range.

As the available pressure is increased the working temperature can decrease, so that cold (room temperature) pressing can achieve theoretical density (0.775 gm/cm^3) at 15,000 to 30,000 psi with 60 mesh powder over a 30 minute cycle. Modern techniques[24] utilize isostatic pressing in a working fluid such as mineral oil with the hydride powder encapsulated by polyvinylchloride (PVC) to prevent sticking. When the piece is extracted from the high pressure cell, the PVC retracts readily and very little contamination of the hydride sample occurs. Usually only small amounts of hydrocarbon plasticizer migrate from the PVC liner into the hydride, and this pollution decreases as the PVC liner is subjected to more use. Chlorine contamination, potentially damaging to the required

x-ray opacity, is essentially nonexistent.

Modern facilities routinely cold press LiH to dimensions equal to or greater than the sizes needed for the structure shown above. If the thin walls of the needed hydride cylinder are difficult to achieve in a PVC capsule, then a thicker walled cylinder can be readily machined down to the needed dimension — provided that the pressing has indeed produced a piece of theoretical density. The squaring of the cylinder's end edges would also be a likely post-pressing requirement. Machining generally gives a surface nearly as smooth as plexiglass[25] which should be adequate for good electrical contact between the copper end rings and the hydride cylinder. While argon atmosphere is typically needed to handle the grinding and transfer of powdered hydride, a nitrogen atmosphere is adequate to support machining of the substance — appreciable formation of nitride contamination doesn't occur below 200 °C .

At a final stage the completed hydride cylinder and end ring could be subjected to a vapor deposition of the interior, metallic Li layer. As an alternative, a metallic Li liner could be included in the cold press stage by placing it to the interior of the LiH charge within the PVC capsule. The use of a liner would require a more precise fitting of the copper end rings to ensure full electrical contact. Roughly speaking, a given thickness of Li metal is equivalent in opacity to two thirds that thickness of LiH because the number of inner shell scatterers is decreased. So the 0.1mm Li interior layer shown in the above design is about the same as 0.067 mm of LiH material, implying that the projected hydride thickness range of 1.5 to 3.0 mm could easily be changed to accomodate the interior conducting surface with no net change in the x-ray transmission.

A sequence of manufacture for hydride return current structures is suggested in Fig. IV.2. Here a charge of powdered LiH is placed in a toroidal PVC bag lined on the interior by a lithium foil or helical strip array. An interior mandrel might be used to support the inner surface of the torus. Once sealed at the end the unit is cold pressed at 30,000 psi to produce a rough structure. Finally excess material is machined away on the exterior and the end rings are pressed into place.

REFERENCES

[1.] Jupiter Design Options Study Team (JDOST) Final Report, SAND94-3163, UC-700 May 1995, vol.I, p.3

[2.] ibid., vol.II, p.271

[3.] E. Nolting, *et al*, DNA PRS Workshop, Apr '95

[4.] W. Rix, ibid.

[5.] A. Fisher, ibid.

[6.] R. Spielman, ibid.

[7.] N. Pereira, ibid.

[8.] N. Pereira, Seminar at NRL, Aug '95

[9.] E. Salberta, DNA PRS Workshop, Apr '95

[10.] D. Mosher, ibid.

[11.] A. Velikovich, BRA Interim Report "Wire Array Implosion Simulation Tool"

[12.] D. LePell, PITR-4742-01, Jan '96

[13.] T. Gibb, C. Messer, AEC Report NYO-3957, Aug '57

[14.] C. Morse, R. Hickel, NASA TND1198 '61

[15.] E. Shpilrain, *et al*,"Thermophysical Properties of Lithium Hydride,. . .", AIP Translation Series, NY '87, p. xi - xv

[16.] ibid., p. 25

[17.] ibid., p. 146

[18.] ibid., p. 150 ff

[19.] F. Biggs, R. Lighthill, "Analytical Approximations to X-ray Cross Sections", SC-RR-710507, Dec '71

[20.] T. Gibb, C. Messer, AEC Report NYO-3957, Aug '57, p.36

[21] ibid., p. 35,37

[22.] R. McKisson, Rport UCRL-992, '50.

[23.] D. Schell, *et al*, "Fabrication of Lithium Hydride by Hot Pressing", LAMS-2108, '58.

[24.] Steve Bidinger, private communication

[25.] Steve Bidinger, private communication

Fig. I.1 Relative Radial Force on a Test Wire

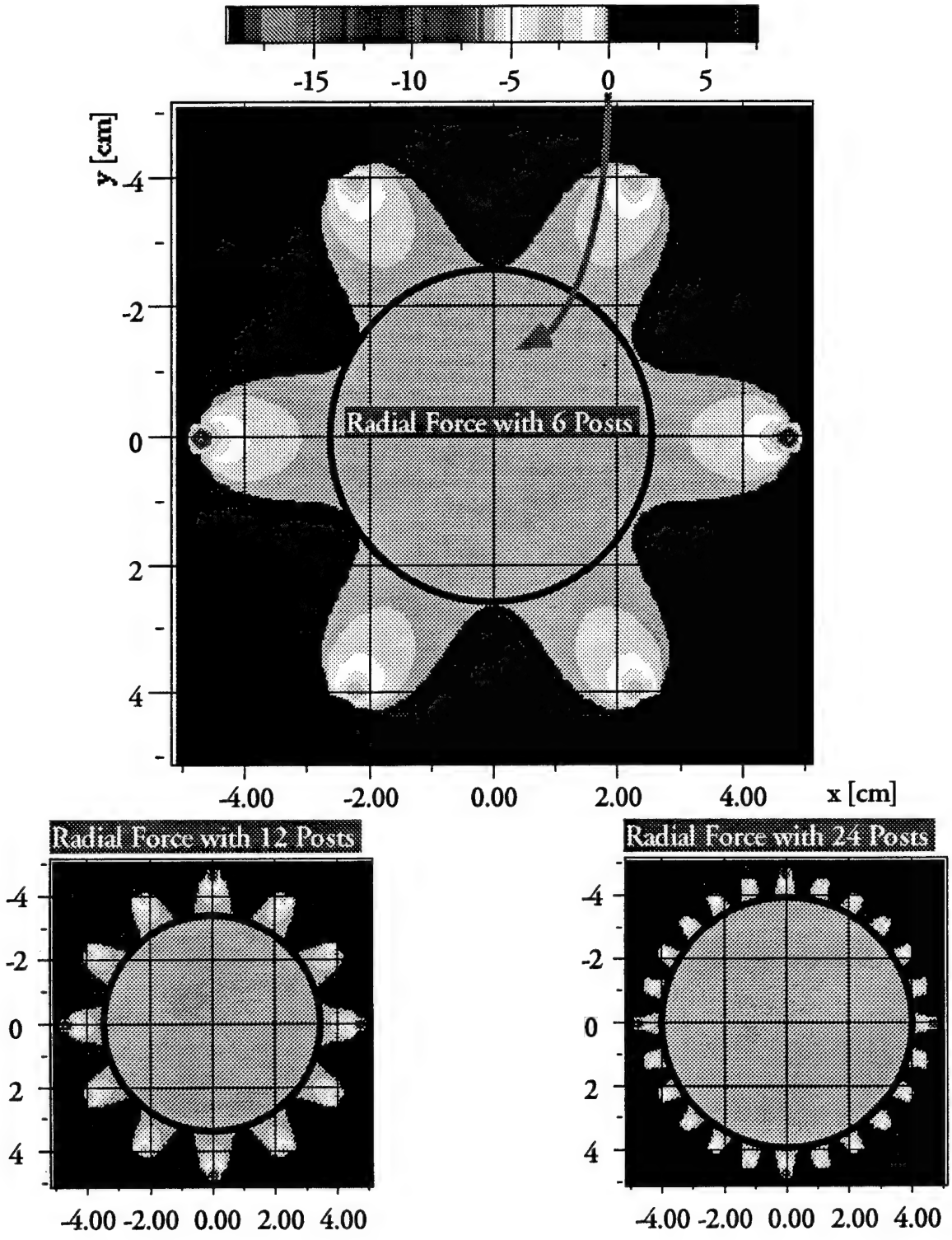

Fig. II.1 LiH Density and Heat Capacity

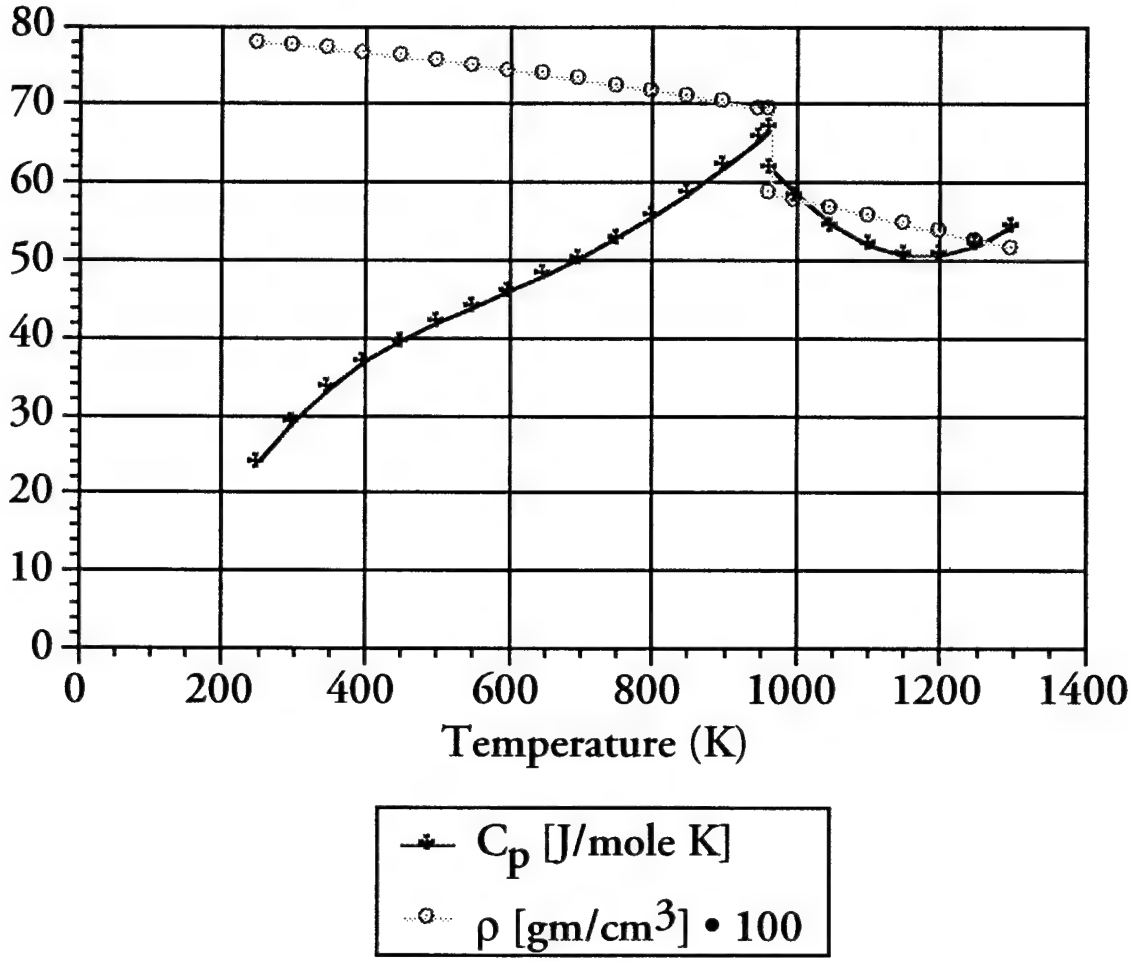

Fig. II.2 LiH Thermal Conduction Coefficient

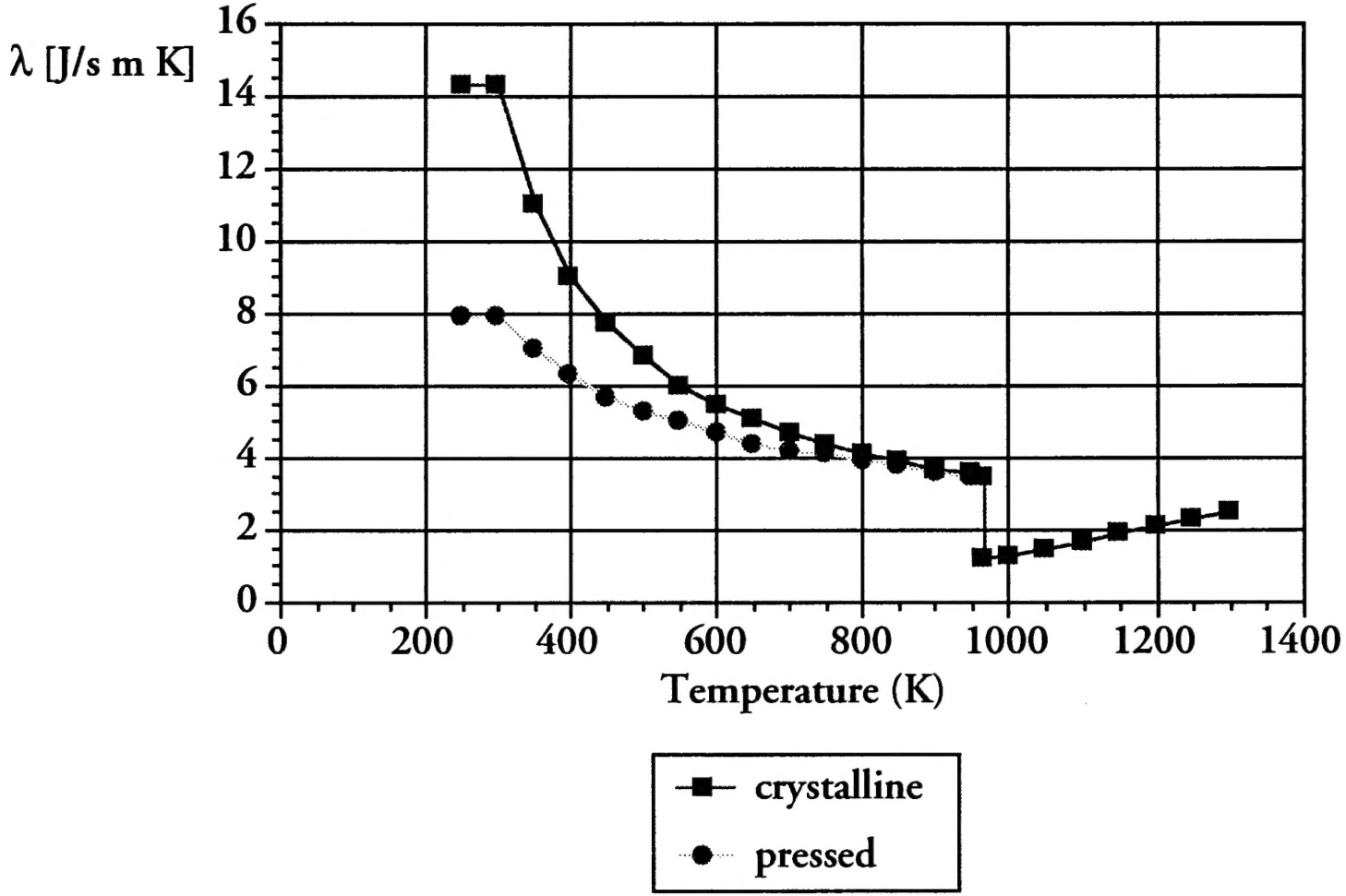

Fig. IV.1a Lithium Hydride —
PRS Debris Shield & Current Return

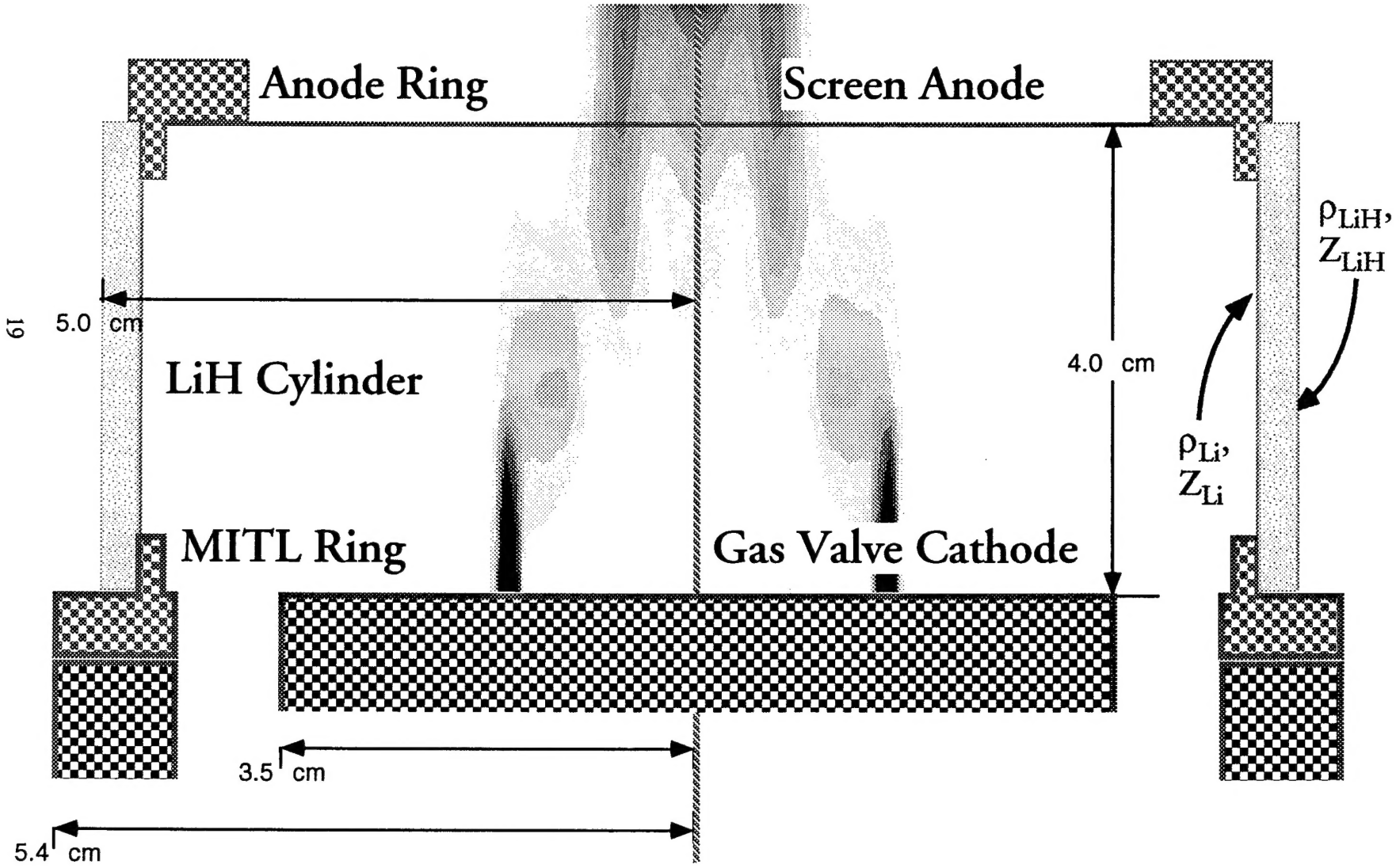

Fig. IV.1b Lithium Hydride —
Optional Twisted Current Return

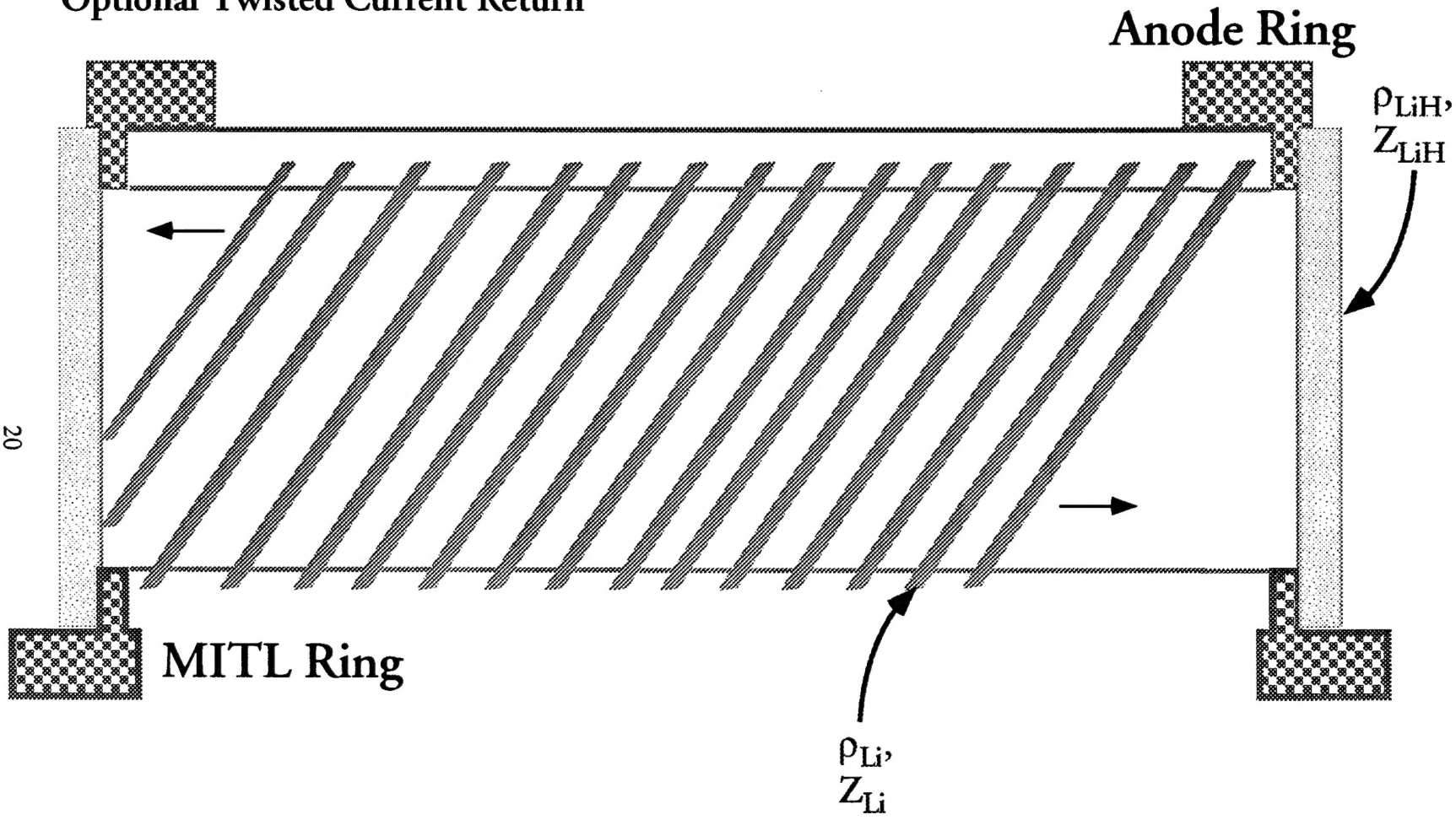

Current return path established in Li strips arranged helically.

Fig. IV.2 MANUFACTURE OF LiH SHIELDS